

An efficient reusable perylene hydrogel for removing some toxic dyes from contaminated water

Ali A Abdulwahid,^a Aula A Alwattar,^{a,b*} Athir Haddad,^{a,b} Mubark Alshareef,^{b,c} Joshua Moore,^b Stephen G Yeates^b and Peter Quayle^b

Abstract

The synthesis of adsorbents that meet the need for large-scale production at relatively low cost and are capable of removing anionic and cationic toxic dyes from aqueous solutions, with high sorption capacity and reusability, is urgently needed from an environmental and industrial viewpoint. In this context the identification of hydrogels that remove dyes efficiently under ambient conditions and at near-neutral pH without the necessity of pre-treatment is an imperative. In this study we report the preparation of two hydrogels using the redox polymerisation of acrylamide, hydroxyethylmethacrylate (HEMA) and *N*-isopropylacrylamide (H1) and acrylamide, HEMA, *N*-isopropylacrylamide and perylene-5-ylpent-3-yne-2-methylprop-2-enoate-co-2-methyl-2-(prop-2-enoylamino)propane-1-sulfonic acid (PePnUMA-co-AMPS) (H2). These hydrogels proved to be effective for the removal of methylene blue (MB), fuchsin acid (FA) and Congo Red (CR) from aqueous solution at near-neutral pH where their adsorption behaviour was in keeping with the Langmuir model having q_{\max} values of 769.2 mg g⁻¹ (MB), 1666.7 mg g⁻¹ (FA) and 2358.2 mg g⁻¹ (CR). The adsorption of MB and FA by these hydrogels follows pseudo-first-order kinetics, whilst the adsorption of CR follows pseudo-second-order kinetics. Detailed thermodynamic analysis indicated that the dye-adsorbent interaction is primarily one of physisorption in nature. Finally, desorption studies carried out in 1.0 mol L⁻¹ NaClO₄ indicated that these adsorbents could be recycled at least four times using a variety of dyes while maintaining their mechanical properties.

© 2021 The Authors. *Polymer International* published by John Wiley & Sons Ltd on behalf of Society of Chemical Industry.

Keywords: dye removal; hydrogel; adsorption kinetics; adsorption isotherms; water treatment

INTRODUCTION

Due to the significant development and scale up of various industrial activities, such as cosmetics, leather, textiles, paper and paint manufacture, enormous quantities of wastewater containing toxic and carcinogenic dyes have been produced as a by-product. In many cases such discharges render groundwater unfit for human consumption^{1,2} or remain present in both raw and treated river water, despite prior effluent treatment by manufacturing facilities.³ These substances pose a threat to human health and have been linked with significant carcinogenic and mutagenic consequences for humans and aquatic species.^{4,5} Dyes are one of the most significant water pollutants that are generated by industrial activities.⁶⁻¹⁰

Therefore, it is of critical importance to remove these dyes prior to discharge into wastewater streams. However, reducing dye content in wastewater streams is not an easy task as dyes are recalcitrant organic compounds and resistant to many treatment methods.¹¹ Numerous studies have used many methods for wastewater treatment, including physical methods, chemical processes and biological activities. These processes include degradation, coagulation, photocatalysis, oxidation, ion exchange and adsorption.¹¹⁻¹³ Adsorption is a more efficient treatment process for removing dyes due to its potential high efficiency, ease of

access,¹⁴ simplicity and wide range of adsorbent availability. Low-cost adsorbents, many of which are themselves waste products,¹⁵⁻¹⁸ have been utilised previously in wastewater management.¹⁹ Because of their relatively low cost of manufacture and high water absorption capacity, polymeric hydrogels are among the best candidates for the development of new adsorbent materials for the removal of heavy metals and dyes.²⁰

Hydrogels are three-dimensional crosslinked polymeric network structures capable of swelling to retain large volumes of water or aqueous fluids due to the inclusion of hydrophilic groups.²¹⁻²³ The specific properties of such gels vary depending upon the

* Correspondence to: A A Alwattar Chemistry Department, the University of Manchester, E-mail: aula.alwattar@manchester.ac.uk. Chemistry Department, College of Science, University of Basrah, Garmat Ali, 61004 Basrah, Iraq. E-mail: ula.jumah@uobasrah.edu.iq

a Chemistry Department, College of Science, University of Basrah, Basrah, Iraq

b Department of Chemistry, University of Manchester, Manchester, UK

c Department of Chemistry, Faculty of Applied Science, Umm Al-Qura University, Makkah, Saudi Arabia

materials used in their synthesis and factors such as degree of crosslinking etc. but are typically characterised as possessing soft 'rubbery' characteristics when hydrated.^{21,24} Their use is widespread in a variety of areas such as tissue engineering, drug delivery systems, agriculture, energy and wastewater treatment.^{25–28} Two hydrogels were used in this study: **H1** as a control gel and **H2**.²²

Methylene blue (MB) is a cationic dye that has several medicinal applications and uses in textile production^{29,30} but has harmful corrosive and irritant effects.³¹ Congo Red (CR) is an anionic dye. Its use has been banned in many countries,³² mainly due to its carcinogenic properties,³³ however, its use persists in printing, paper, rubber and textile production.^{15,34} Fuchsin acid (FA) is an acidic dye, commonly used in bacterial staining.³⁵ Treatment of wastewater containing FA has received significant attention due to its toxicity.³⁶ Xing *et al.* report a hydrogel formulated from gelatin, carboxymethyl cellulose and polypyrrole with exclusive FA adsorption at 94% removal efficiency. This removal efficiency remained unchanged over seven cycles of adsorption/desorption.³⁷

Jana *et al.*¹⁹ used acrylamide, *N,N*-dimethylacrylamide and hydroxyl ethyl cellulose hydrogel for the removal of CR; the adsorption followed pseudo-second-order kinetics, and the Langmuir adsorption isotherm was well suited to the sorption data. The hydrogel showed a high adsorption capacity (102.4 mg g⁻¹).

The isothermal studies of FA removal by modified zeolite showed that the adsorption was fitted well by the Langmuir isotherm with an adsorption capacity up to 31.0 mg g⁻¹ while thermodynamic parameters indicated that the adsorption of FA using modified zeolites was exothermic.³⁸ The adsorption of MB onto poly(vinyl alcohol)-xanthan gum hydrogels displayed second-order kinetics and the Langmuir sorption isotherm.³⁹ A hydrogel that was formulated from 3-acrylamidopropyltrimethyl ammonium chloride and 2-acrylamido-2-methylpropanesulfonic acid was used for the removal of crystal violet (CV) and CR dyes in an aqueous medium and it was found to be more selective and efficient at pH 5.0 and 9.0 for CR and CV, respectively.⁴⁰

The formulations of new hydrogels derived from poly(acrylic acid), sodium humate and sodium alginate were investigated as efficient and selective adsorbents for MB and CV dyes. The binding capacities of these dyes were 367.0 and 359.0 mg g⁻¹, respectively, and the absorption was fitted well with the Langmuir sorption isotherm.⁴¹

The current study involves the preparation of interpenetrating polymer network (IPN) hydrogel **H1** from acrylamide with hydroxyethyl methacrylate (HEMA) as a control and IPN hydrogel **H2** from the same components and perylene-5-ylpent-3-yn-2-methylprop-2-enoate-co-2-methyl-2-(prop-2-enoylamino)propane-1-sulfonic acid (PePnUMA-co-AMPS). The prepared hydrogel **H2** was fully characterised and used in our previous work to sequester toxic, heavy metals from aqueous solutions.⁴² In the present study, **H2** is also used to remove organic dyes: methylene blue (MB), fuchsin acid (FA) and congo red (CR). It was found that **H2** exhibited good efficiency for removing these dyes.

MATERIALS AND METHODS

Chemicals

All reactants, reagents and dry solvents were purchased from Merck (Watford, Hertfordshire, United Kingdom), Acros Organics and Fisher Scientific (Loughborough, United Kingdom) and were used without further purification except for 2,2'-azobis(2-methylpropanionitrile) which was recrystallised from methanol and *N*-bromosuccinimide which was purified by recrystallisation from

water prior to use. All glassware was heated in vacuum before use and all reactions were performed under nitrogen gas. Thin-layer chromatography (TLC) was carried out using DC-Fertigfolie POLY-GRAM® SIL G/UV254 precoated TLC sheets with substrate detection by UV light (254 and 365 nm).

Synthesis

Synthesis of the monomer and copolymer

5-(Perylene-3-yl)pent-4-yn-1-yl methacrylate (PePnUMA) (monomer) and PePnUMA-co-AMPS were synthesised and fully characterised according to our previously reported procedure.^{42–44}

Preparation of IPN hydrogels **H1** and **H2**

H1 (control) was prepared by dissolving acrylamide (5.0 g), HEMA (2.0 g) and methylene *N,N'*-methylenebis(acrylamide) (0.72 g) as a crosslinker in 15 mL deionised (DI) water. To this homogeneous solution was then added ammonium persulphate (200 µL of a 10% w/v aqueous solution) as initiator and *N,N,N',N'*-tetramethylethylenediamine (25 µL) as an accelerator for initiator decomposition and the reaction mixture was stirred at room temperature for 10 min in order for the polymerisation reaction to go to completion. This process was repeated for the hydrogel **H2** with the same components and PePnUMA-co-AMPS (0.2 g). The resulting hydrogels were dried and washed three times with DI water to remove any monomer residue, filtered and dried under vacuum (1 Torr) at 25 °C for 24 h.

Preparation of aqueous dye solutions

Stock dye solutions were prepared by dissolving 1.0 g of each dye (MB, FA and CR) in DI water (1 L) to give a concentration of 1.0 g L⁻¹. Successive dilutions of these dye stock solutions in DI water were then used to obtain the working concentrations (40.0, 250.0 and 600.0 mg L⁻¹ solution of MB, FA and CR respectively). The molecular structures and λ_{\max} of these dyes and of PePnUMA-co-AMPS are shown in Table 1.

Batch adsorption experiments

Batch adsorption experiments of MB, FA and CR were carried out to evaluate the adsorption parameters and factors influencing the adsorption. A total of 25.0 mg of adsorbents **H1** and **H2** were placed in 100 mL solutions (40.0, 250.0 and 600.0 mg L⁻¹ solution of MB, FA and CR respectively). The adsorption experiments were conducted on a thermostat shaker at 25 °C, and the adsorption media was stirred magnetically at 225 rpm for a specific period of time (15–90 min). After adsorption, the adsorbent was separated from the solution by simple filtration. The concentration of dye was determined by UV-visible spectroscopy at the λ_{\max} of each dye. UV-visible spectra were recorded using a T80⁺ spectrophotometer between 200 and 800 nm using a quartz cuvette with a path length of 1 cm.

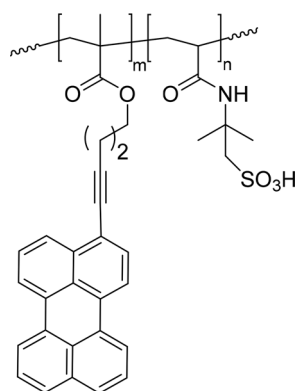
Adsorption experiments were carried out at optimum conditions applying an agitation time of 60, 15 and 90 min at pH 9.0, 5.0 and 7.0 for MB, FA and CR respectively. The concentration of these dyes on **H1** and **H2** adsorbent hydrogels was calculated using the following equation:^{45,46}

$$q_e = \frac{C_0 - C_e}{w} V \quad (1)$$

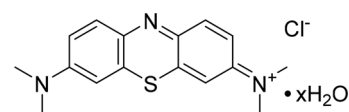
where C_0 and C_e (mg L⁻¹) are the initial and equilibrium concentration of dye in the solution, V (L) is the volume of solution, w (g) is the mass of hydrogel and q_e is the adsorption capacity (mg dye per g hydrogel).

Table 1. Molecular structure of the prepared copolymer PePnUMA-co-AMPS and MB, FA and CR

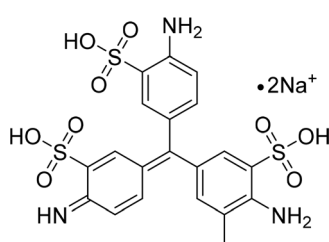
PePnUMA-co-AMPS

 $\lambda_{\max} = 460 \text{ nm}$ 

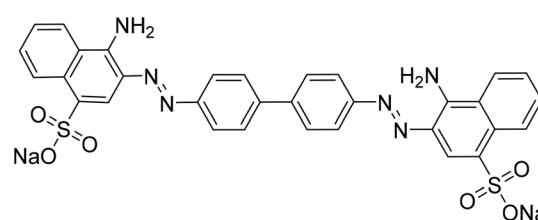
Methylene blue

 $\lambda_{\max} = 665 \text{ nm}$ 

Fuchsin acid

 $\lambda_{\max} = 545 \text{ nm}$ 

Congo Red

 $\lambda_{\max} = 498 \text{ nm}$ 

In order to study the adsorption kinetics and to calculate the kinetic parameters enthalpy (ΔH°), entropy (ΔS°) and free energy (ΔG°), experiments were conducted at 25, 45 and 65 °C using 25 mg of **H1** and **H2** in 100 mL solutions of 40, 250 and 600 mg L⁻¹ of MB, FA and CR respectively. By varying the pH of the dye solutions from 1 to 14, the maximum adsorption capacity was found at optimum pH. The pH of the dye solutions was adjusted using 0.1 mol L⁻¹ solutions of HCl and NaOH.

The desorption of dyes from the hydrogels was carried out by applying five adsorption/desorption cycles of the same adsorbent. The maximum dye adsorption was accomplished by applying the optimum agitation time and pH for each dye-hydrogel combination. The desorption experiments were carried out by immersing dye-loaded adsorbent into a 1.0 mol L⁻¹ solution of NaClO₄, and the mixture was stirred at 25 °C for 45 min. The desorbed dyes were then separated by centrifugation and filtration. The concentration of the dye in each solution was determined spectrophotometrically.^{39–41} The removal efficiency of the MB, FA and CR dyes was calculated using⁴⁷

$$S(\%) = \frac{C_d V_d}{q_e W} \times 100\% \quad (2)$$

where *S* is the efficiency of dye desorption, *C_d* is the dye concentration in solution after desorption (mg L⁻¹) and *V_d* is the volume of the eluent (L).

RESULTS AND DISCUSSION

The synthesis of the PePnUMA monomer, the corresponding PePnUMA-co-AMPS polymer network (1:30 monomer feed ratio) and the fabrication of semi-IPN hydrogels were attempted using our previously reported procedure.⁴⁸ From our previous work these systems have good chemical and thermal stability and show efficient detection and removal of heavy metal ions (e.g. Co²⁺, Cu²⁺, Ni²⁺, Hg²⁺ and Pb²⁺) from aqueous media at neutral pH at room temperature.

The adsorption performance of **H1** and **H2** towards MB, FA and CR dyes was investigated by using batch system experiments at optimum pH, contact time, temperature and initial concentration (*C*₀) for each dye.

The important parameter influencing the hydrogel's adsorption capability is pH. The effect of pH on dye adsorption capacity using these hydrogels was measured between pH 1.0 and pH 14.0. Figures 1(A)–1(C) illustrate the influence of the variation of pH on the adsorption capacities of **H1** and **H2**. Figure 1(A) shows that the adsorption capacities of **H1** and **H2** increase with increased pH for cationic dye MB and decrease with increased pH for anionic dyes. In the case of the cationic dye MB the electrostatic attraction between MB and the ionised sulfonic acid and phenolic groups present in the hydrogel at alkaline pH favour adsorption of the dye onto the hydrogel surface.^{49–51}

In the same way, the optimum pH value is 5.0 for FA adsorption; however, at low pH more H⁺ ions are available, thereby increasing

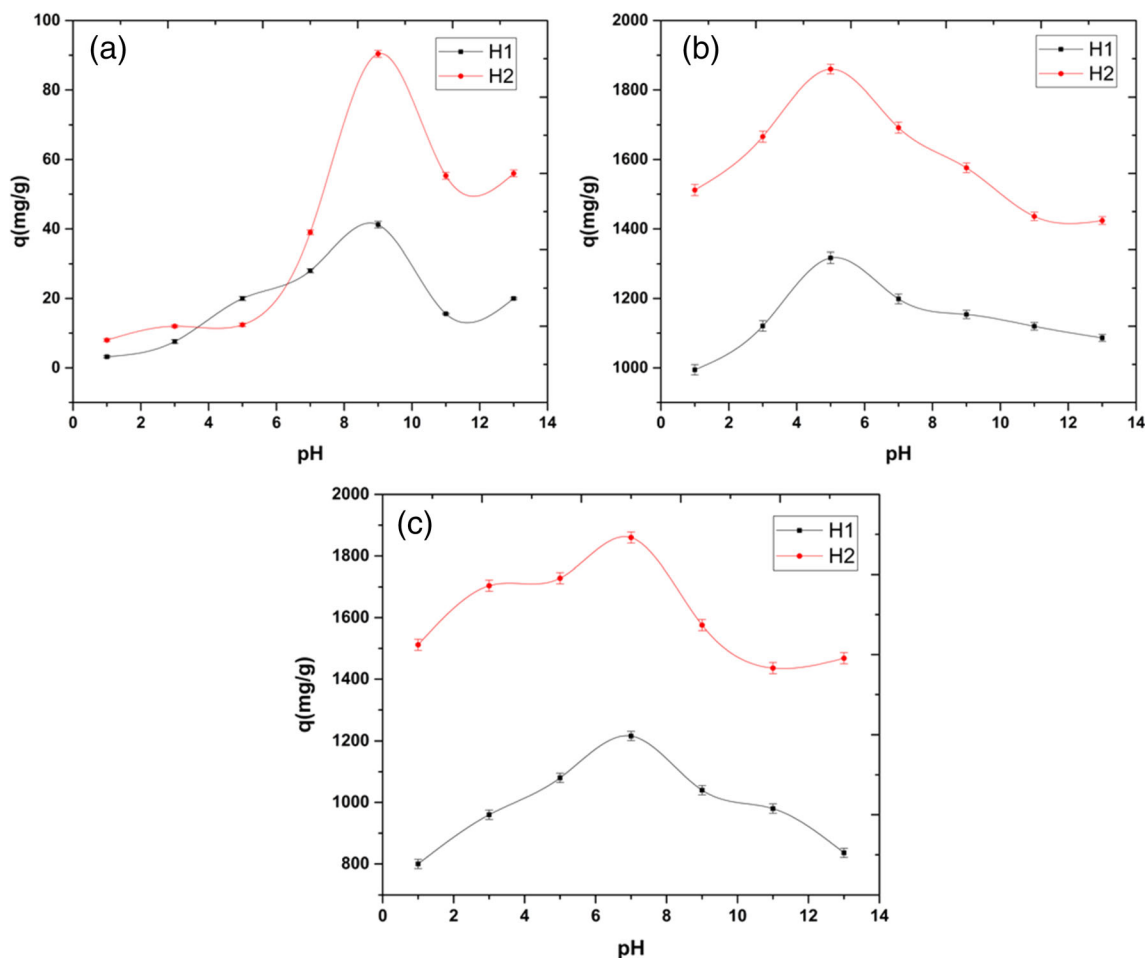


Figure 1. Effect of pH on the adsorption of hydrogels **H1** and **H2**: (A) MB, (B) FA and (C) CR dyes.

electrostatic attractions between negatively charged FA and CR dye anions and positively charged adsorption sites. This is due to the protonation of the $-\text{CONH}_2$ group which leads to an increase in the adsorption capacity.¹⁹ Also, the abundance of OH^- ions at high pH may cause an ionic repulsion between the negatively charged surface and the anionic dye molecules.

The determination of optimum contact or agitation time⁵² was carried out at diverse dye initial concentrations ($20.0\text{--}700.0\text{ mg L}^{-1}$) and the best initial concentrations of MB, FA and CR dyes on **H1** and **H2** were found to be 40.0 , 250.0 and 600.0 mg L^{-1} respectively.

Figures 2(A)–2(C) show the plots for the effect of agitation time for the adsorption of MB, FA and CR dyes at pH 9.0, 5.0 and 7.0, respectively, onto adsorbent hydrogels at different temperatures. The adsorption of MB increased rapidly from 1 to 30 min; the adsorption capacity increases as the temperature increases (from 25 to 65 °C) and the equilibrium attained within 60–150 min suggests an endothermic process. Figures 2(B) and 2(C) show the adsorption equilibrium times for FA and CR to be 15 and 90 min respectively. Since the adsorption of MB, FA and CR is endothermic, this tendency for the adsorption capacities of the adsorbent was expected. Thus, the optimum agitation times for all further experiments were chosen as 15, 60 and 90 min for the adsorption of MB, FA and CR dyes respectively.

A comparison of the maximum adsorption capacity of **H2** with some reported adsorbents in the literature^{37,53–59} for the removal

of toxic dyes is summarised in Table 2. The results in this table show that the values of adsorption capacity of **H2** are much better than some other reported adsorbents. This indicates that **H2** is an excellent adsorbent and can be used for the removal of dyes from aqueous media.

Figure 3(A) shows the effect of pH on the adsorption capacity (q) of dyes onto hydrogels **H1** and **H2** while Fig. 3(B) shows the effect of temperature on the adsorption capacity (q) of dyes onto hydrogels **H1** and **H2**.

These results indicate high adsorption efficiency of the hydrogel **H1** due to the electrostatic interaction between the dyes and the hydrogel **H1**, while hydrogel **H2** showed much higher adsorption efficiency. This observation can be rationalised by the presence of the large, polycyclic, aromatic residues which are embedded within the newly synthesised hydrogel which enables π – π stacking between the aromatic core of the polymer PePnUMA-co-AMPS and the dye molecules in a process that is augmented by H-bonding.^{61–63}

To further comprehend the adsorption and explore the adsorption process mechanism, the adsorption equilibrium isotherms between adsorbents and adsorbate were studied at a fixed temperature of 25 °C. Adsorption data are generally described by adsorption models, such as the Langmuir and Freundlich isotherms. The Langmuir is illustrated by the following equation:³⁹

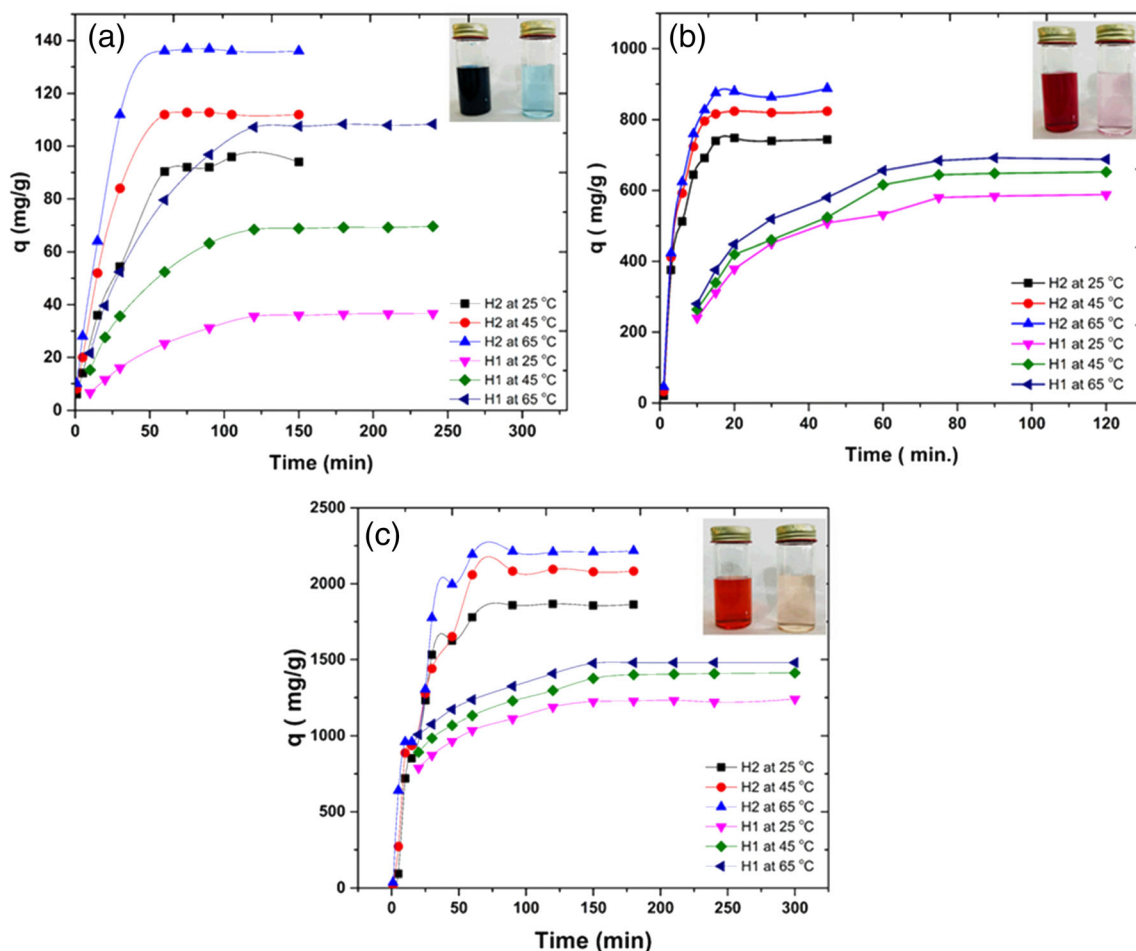


Figure 2. Effect of time on the adsorption of dyes by hydrogels **H1** and **H2**: (A) MB at pH 9.0, (B) FA at pH 5.0 and (C) CR at pH 7.0 as a function of temperature. The bottles show the dye solutions before (left) and after (right) adsorption.

Table 2. Comparison of maximum adsorption capacities of MB, AF and CR onto **H2** hydrogel adsorbent and other adsorbents

Adsorbent	Dye	Adsorption capacity (mg g ⁻¹)	Reference
Carboxymethyl sago pulp-sago waste	MB	158.0	59
Polyacrylamide-phytic acid-polydopamine	MB	350.7	58
2-Acrylamide-2-methylpropanesulfonic acid	MB	434.8	57
Sulfonated poly(arylene ether nitrile)- aluminium(III) ions	MB	699.3	56
Carboxymethyl cellulose-gelatin-polypyrrole	FA	17.6	37
Cetyl trimethyl ammonium bromide-chitosan	CR	433.1	55
Cetyl trimethyl ammonium bromide	CR	263.2	60
Chitosan hydrobeads	CR	93.4	53
H2	MB	769.2	This study
	FA	2358.2	
	CR	1666.7	

$$\frac{C_e}{q_e} = \frac{1}{q_{\max} K_L} + \frac{C_e}{q_{\max}} \quad (3)$$

where C_e (mg L⁻¹) is the dye concentration remaining in solution at equilibrium, q_e (mg g⁻¹) is the equilibrium concentration of dye adsorbed by the hydrogel, K_L (L mg⁻¹) is the Langmuir adsorption constant and q_{\max} (mg g⁻¹) is the monolayer adsorption capacity of

the hydrogel. The slope of the plot of C_e/q_e versus C_e is equal to $1/q_{\max}$ and the Y intercept is equal to $1/q_{\max}K_L$. The Langmuir equation is valid for monolayer adsorption of dye (adsorbate) onto the hydrogel surface (adsorbent), and it assumes that there are restricted and homogeneous adsorption sites.⁶⁴ The essential characteristics of a Langmuir isotherm can be expressed in terms of a dimensionless constant separation factor or equilibrium parameter R_L which is defined as⁶⁵

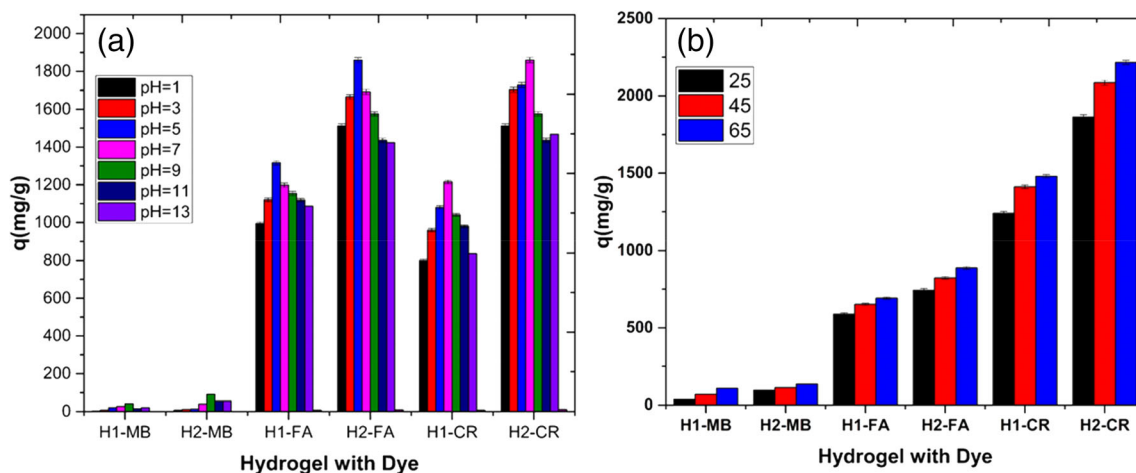


Figure 3. The effect of pH (A) and temperature (B) on the adsorption capacity (q) of dyes onto hydrogels **H1** and **H2**: MB concentration 40.0 mg L^{-1} at pH 9.0; FA concentration 250.0 mg L^{-1} at pH 5.0; CR dye concentration 600.0 mg L^{-1} at pH 7.0.

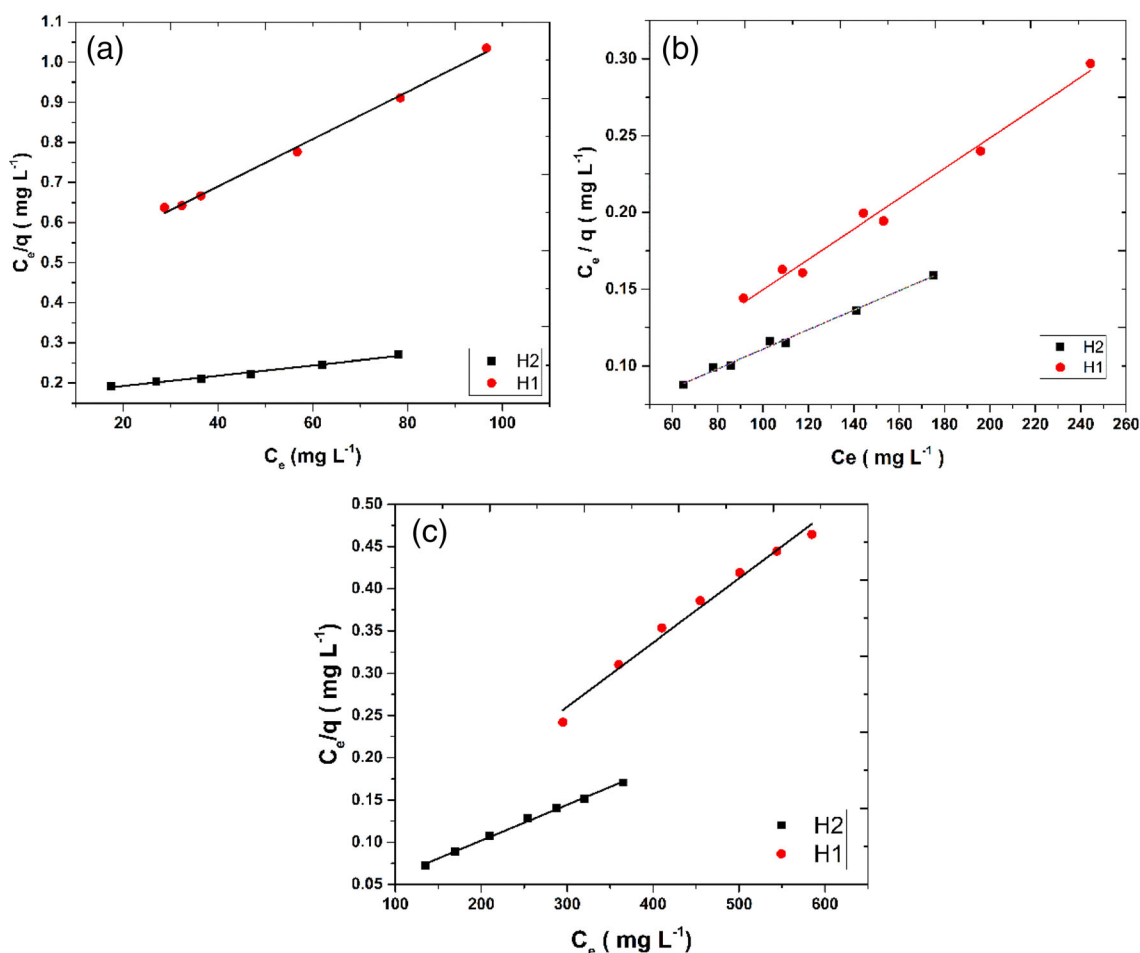


Figure 4. Langmuir isotherm model for the adsorption of (A) MB (concentration 40.0 mg L^{-1} at pH 9.0), (B) FA (concentration 250.0 mg L^{-1} at pH 5.0) and (C) CR (concentration 600.0 mg L^{-1} at pH 7.0) by hydrogels **H1** and **H2**.

$$R_L = \frac{1}{1 + K_L C_0} \quad (4)$$

where K_L is the Langmuir constant and C_0 is the initial concentration.

The type of isotherm can be determined by R_L values which indicate whether a sorption system is favourable ($0 < R_L < 1$) or unfavourable ($R_L > 1$). Figures 4(A)–4(C) give plots of the Langmuir adsorption isotherms of MB, FA and CR adsorbed onto hydrogels **H1** and **H2**. Table 2,3 displays q_{max} , K_L , R^2 and the correlation

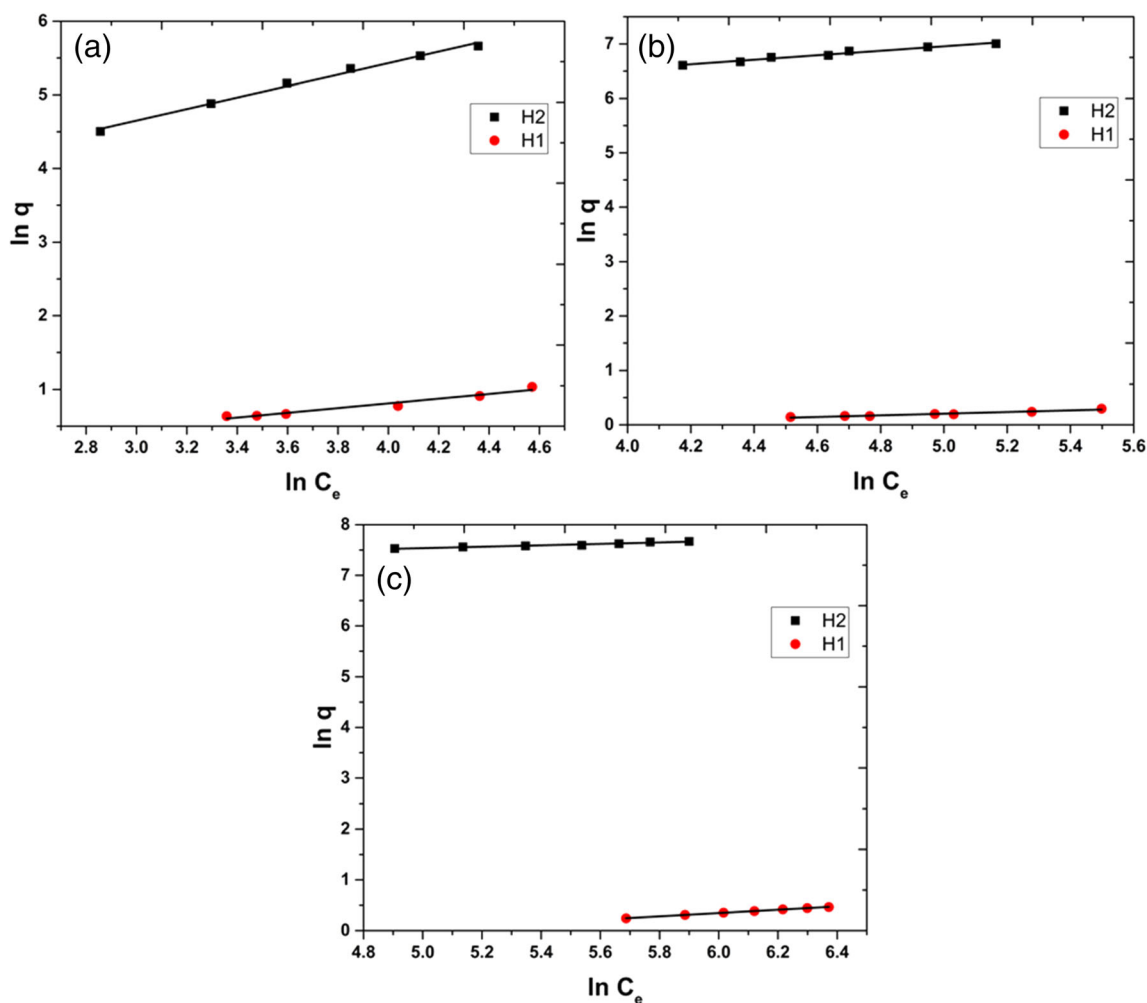


Figure 5. Freundlich isotherm model for (A) MB (concentration 40.0 mg L⁻¹ at pH 9), (B) FA (concentration 250.0 mg L⁻¹ at pH 5) and (C) CR (concentration 600.0 mg L⁻¹ at pH 7.0) adsorbed onto hydrogels **H1** and **H2**.

Table 3. Langmuir and Freundlich isotherm parameters for the adsorption of MB, FA and CR dyes onto **H1** and **H2** at 25 °C

Dye	Hydrogel	Langmuir isotherm			Freundlich isotherm		
		q_{\max} (mg g ⁻¹)	K_L (L mg ⁻¹)	R^2	K_F (L mg ⁻¹)	$1/n$	R^2
MB	H1	169.492	0.0130	0.9963	1.608	0.3213	0.9601
MB	H2	769.230	0.0078	0.9926	10.080	0.7802	0.9811
FA	H1	1010.101	0.0195	0.9878	1.739	0.1517	0.9521
FA	H2	1666.667	0.0127	0.9929	133.501	0.4123	0.9761
CR	H1	1315.789	0.0237	0.9841	5.011	0.3263	0.9993
CR	H2	2358.21	0.0002	0.9970	924.362	0.1414	0.9557

coefficient results for the Langmuir isotherms. The calculated R_L values of the dyes MB, FA and CR onto **H1** and **H2** are found to be 0.762, 0.240 and 0.893 respectively at initial dye (MB, FA and CR) concentrations of 40.0, 250.0 and 600.0 mg L⁻¹ respectively. These results indicate that these hydrogels are favourable for adsorbing dyes from aqueous solutions under the optimised conditions applied in this study.

The Freundlich isotherm is based on a heterogeneous exponentially decaying distribution, which fits well to the tailing portion of the heterogeneous distribution of the adsorbent. The general Freundlich isotherm can be defined as⁴¹

$$\ln q_e = \ln K_F + \frac{1}{n} \ln C_e \quad (5)$$

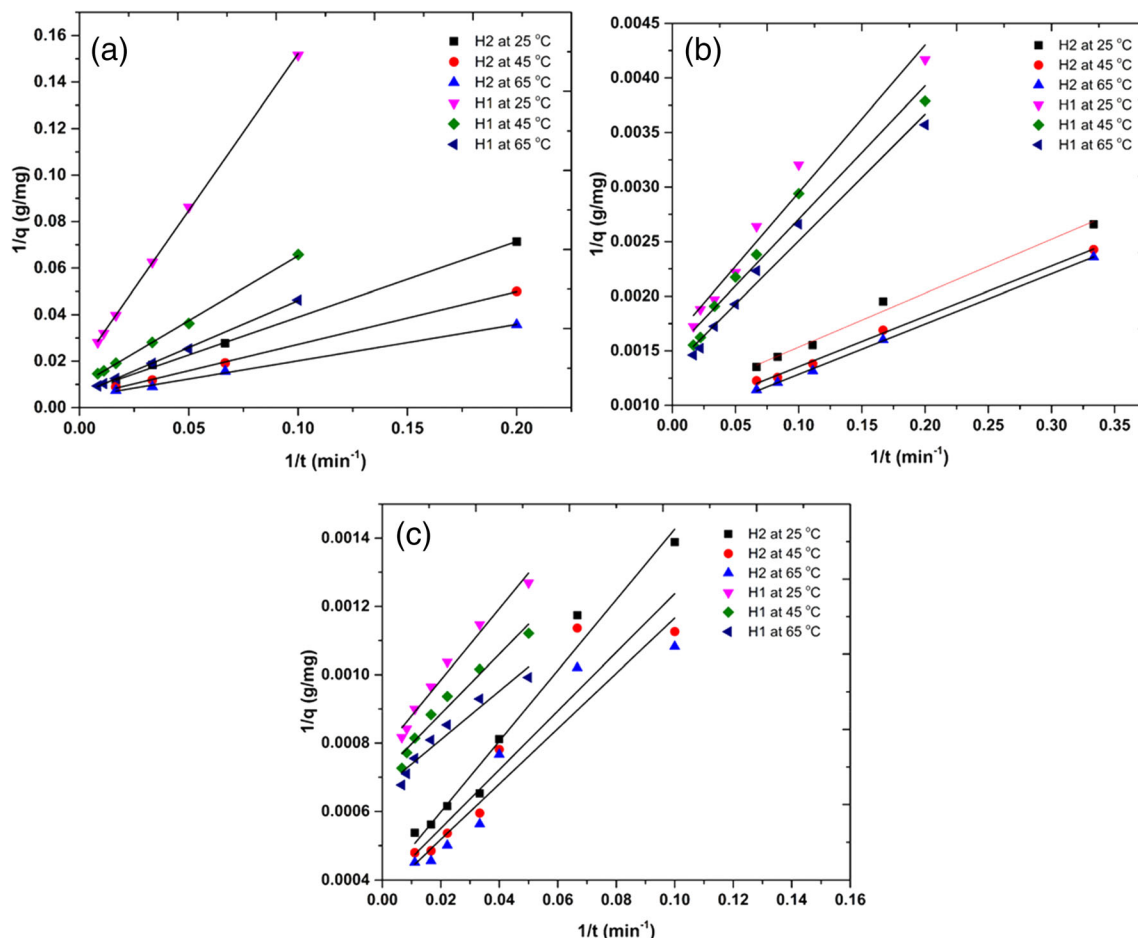


Figure 6. Pseudo-first-order kinetic plots for the adsorption of (A) MB (concentration 40.0 mg L⁻¹ at pH 9.0), (B) FA (concentration 250.0 mg L⁻¹ at pH 5.0) and (C) CR (concentration 600.0 mg L⁻¹ at pH 7.0) onto **H1** and **H2** hydrogels at different temperatures.

where K_F (L mg⁻¹) is a constant for the adsorption or distribution coefficient and represents the amount of dye adsorbed onto the hydrogel at equilibrium concentration. Figures 5(A)–5(C) show plots of the Freundlich adsorption isotherms of MB, FA and CR adsorbed onto the hydrogels. Table 3 displays also K_F , $1/n$ and the correlation coefficients which were determined from the linear plot of $\ln q_e$ versus $\ln C_e$.

Table 3 shows the linearity of the Langmuir isotherm equation, which resulted in an improved fit compared to that of the Freundlich isotherm equation for MB, FA and CR dyes despite the complexity of the adsorption processes. However, this could suggest that there was a tendency for chemical adsorption to exist between functional groups of hydrogel **H2** and the dyes. The values of $1/n$ were obtained from the slopes of the Freundlich isotherm plots in Fig. 5 for MB, FA and CR, and are below 1. These values are indicative of normal Langmuir isotherm behaviour of dye adsorption processes onto the **H2** hydrogel.⁶⁶

Three kinetic models were tested to interpret the mechanism of adsorption of MB, FA and CR dyes onto the prepared hydrogels. The first model was pseudo-first-order; the mathematical expression of this model is given by⁶⁷

$$\frac{1}{q_t} = \frac{K_1}{q_1 t} + \frac{1}{q_1} \quad (6)$$

where q_t and q_1 (mg g⁻¹) are the amounts of dye adsorbed at time t and at equilibrium and K_1 (min⁻¹) is the pseudo-first-order rate adsorption constant.

A plot of $1/q_t$ versus $1/t$ gives the rate constants (K_1) and correlation coefficients. Figures 6(A)–6(C) represents the pseudo-first-order equations for MB, FA and CR dyes at different temperatures and the calculated K_1 and q_1 values are shown in Table 3,4.

The second kinetic model was pseudo-second-order, which can be represented by the following equation:^{49–52}

$$\frac{t}{q_t} = \frac{1}{K_2 q_2^2} + \frac{1}{q_2} t \quad (7)$$

where q_2 is the maximum adsorption capacity (mg g⁻¹) for pseudo-second-order adsorption and K_2 (g mg⁻¹ min⁻¹) is the equilibrium rate constant for pseudo-second-order adsorption. Values of q_2 and K_2 were calculated from the slope and Y intercept of the plot of t/q_t versus t (Figs 7(A)–7(C)). The kinetic data for the adsorption of MB, FA and CR dyes onto the prepared hydrogels at various temperatures were calculated from the related plots and are summarised in Table 4.

Intra-particle diffusion was the final model investigated in this study; the intra-particle diffusion model equation is shown as^{49–52,61}

$$q_t = K_p t^{1/2} + C \quad (8)$$

where C is the Y intercept and K_p is the intra-particle diffusion rate constant (mg⁻¹ min^{-1/2}) which were calculated from the slope of the plot of q_t versus $t^{-1/2}$. Figure 8 displays the intra-particle

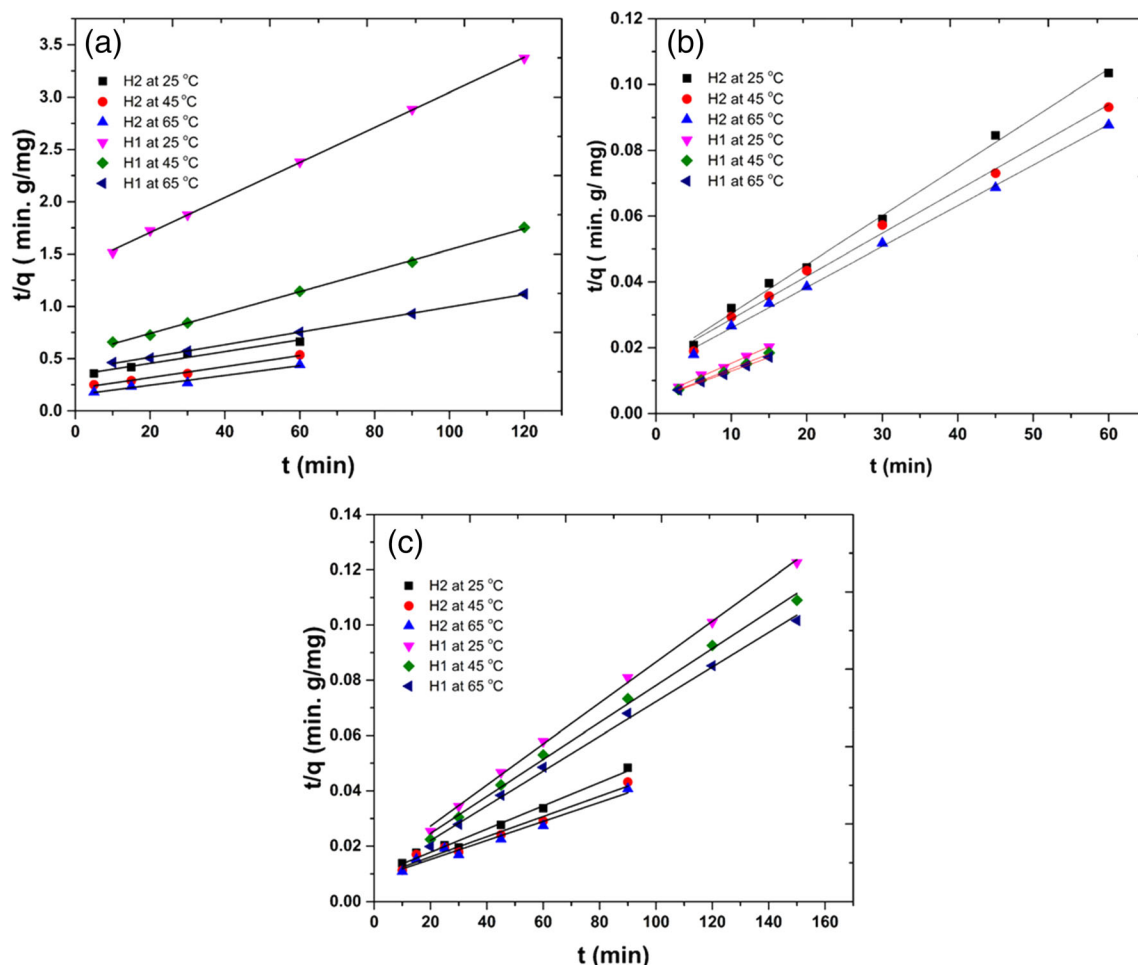


Figure 7. Variation of pseudo-second-order kinetic plots for the adsorption of (A) MB (concentration 40.0 mg L⁻¹ at pH 9.0), (B) FA (concentration 250.0 mg L⁻¹ at pH 5.0) and (C) CR (concentration 600.0 mg L⁻¹ at pH 7.0) onto **H1** and **H2** hydrogels with temperature.

diffusion model for MB, FA and CR dyes at different temperatures and Table 4 shows the calculated K_p and C values.

As is evident from the correlation coefficients in Table 4, the MB and FA dye adsorption systems follow the pseudo-first-order model and K_1 values increase with increase in temperature, while CR adsorption follows a pseudo-second-order model. However, the K_2 values were not always directly proportional to temperature.

Thermodynamic parameters can be determined from the thermodynamic equilibrium constant K_L (or the thermodynamic distribution coefficient) and are expressed in the following equation:⁶⁷

$$K_L = \frac{C_a}{C_e} \quad (9)$$

where C_a and C_e are the equilibrium concentrations of MB, FA and CR dyes onto **H1** and **H2**, as an adsorbent (mg g⁻¹) and in the solution (mg L⁻¹) respectively.

The standard enthalpy change ΔH° (kJ mol⁻¹) and the standard entropy change ΔS° (J mol⁻¹ K⁻¹) were calculated using the following equation:^{39,67}

$$\ln K_L = \frac{\Delta S^\circ}{R} - \frac{\Delta H^\circ}{RT} \quad (10)$$

where R is the universal gas constant (8.314 J mol⁻¹ K⁻¹) and T is the absolute temperature. ΔH° was obtained from the slope of

the plot of $\ln K_L$ versus $1/T$ (K⁻¹) and ΔS° was obtained from the Y intercept for the adsorption of MB, FA and CR dyes. The standard Gibbs free energy ΔG° (kJ mol⁻¹) was calculated at different temperatures, as listed in Table 5, from the following equation:^{39,49,67}

$$\Delta G^\circ = \Delta H^\circ - T\Delta S^\circ \quad (11)$$

The activation energy E_a (kJ mol⁻¹), which is defined as the minimum amount of energy required in order for the adsorption process to proceed, was calculated from the Arrhenius equation:^{39,49,67}

$$\ln K = \ln A - \frac{E_a}{RT} \quad (12)$$

where K is the rate constant of the pseudo-first-order kinetic model (min⁻¹) for the adsorption system of MB and FA dyes whereas it is pseudo-second-order (g mg⁻¹ min⁻¹) for the adsorption system of CR, (this is based on R2 result). A is the Arrhenius factor, when $\ln K$ is plotted versus $1/T$, a straight line with slope $-E_a/R$ is obtained. Table 5 lists the E_a values for the adsorption of MB, FA and CR.

The calculated thermodynamic parameters listed in Table 5 show negative values of enthalpy changes (ΔH°) for all dyes,

Table 4. Kinetic parameters for the adsorption of MB, FA and CR dyes onto **H1** and **H2** at constant pH and different temperatures

Dye/gel	T (°C)	Pseudo-first-order			Pseudo-second-order			Intra-particle diffusion		
		K_1 (min ⁻¹)	q_1 (mg g ⁻¹)	R_1^2	K_2 (g mg ⁻¹ min ⁻¹)	q_2 (mg g ⁻¹)	R_2^2	K_p (mg g ⁻¹ min ^{-1/2})	C	R_p^2
MB/H1	25	77.494	57.47	0.9997	2.0×10^{-4}	59.88	0.9996	3.781	-4.99	0.9971
	40	58.010	104.17	0.9990	1.9×10^{-4}	100.00	0.9989	6.890	-3.69	0.9854
	55	69.379	172.41	0.9994	9.2×10^{-5}	166.67	0.9994	11.100	-10.20	0.9913
MB/H2	25	50.797	156.25	0.9991	9.2×10^{-5}	178.57	0.9618	13.730	-17.66	0.9956
	40	49.174	217.39	0.9994	1.3×10^{-4}	188.68	0.9924	16.811	-14.25	0.9860
	55	54.000	344.83	0.9977	1.5×10^{-4}	212.77	0.9784	20.170	-12.49	0.9601
FA/H1	25	8.438	625.00	0.9735	1.4×10^{-4}	671.14	0.9965	61.324	133.79	0.9396
	40	8.133	666.67	0.9675	1.1×10^{-4}	769.23	0.9945	70.377	128.30	0.9789
	55	8.923	769.23	0.9830	1.1×10^{-4}	806.45	0.9980	74.026	150.00	0.9609
FA/H2	25	4.744	960.80	0.9909	2.0×10^{-4}	993.25	0.9959	17.380	8.81	0.9792
	40	5.165	1119.33	0.9976	1.8×10^{-4}	1105.30	0.9964	19.531	10.09	0.9616
	55	5.586	1213.15	0.9994	1.5×10^{-4}	1201.30	0.9991	21.324	8.32	0.9724
CR/H1	25	13.397	1282.05	0.9772	4.5×10^{-5}	1351.35	0.9987	55.779	571.35	0.9771
	40	12.324	1408.45	0.9609	4.2×10^{-5}	1449.28	0.9968	59.94	650.55	0.9914
	55	10.612	1492.54	0.9416	4.2×10^{-5}	1587.30	0.9971	59.602	756.74	0.9946
CR/H2	25	26.447	2554.74	0.9729	1.9×10^{-5}	2380.39	0.9856	189.89	246.91	0.8804
	40	22.677	2640.89	0.8856	1.5×10^{-5}	2737.70	0.9676	219.26	235.26	0.8765
	55	22.717	2806.31	0.9155	1.4×10^{-5}	2909.68	0.9683	233.89	241.20	0.8790

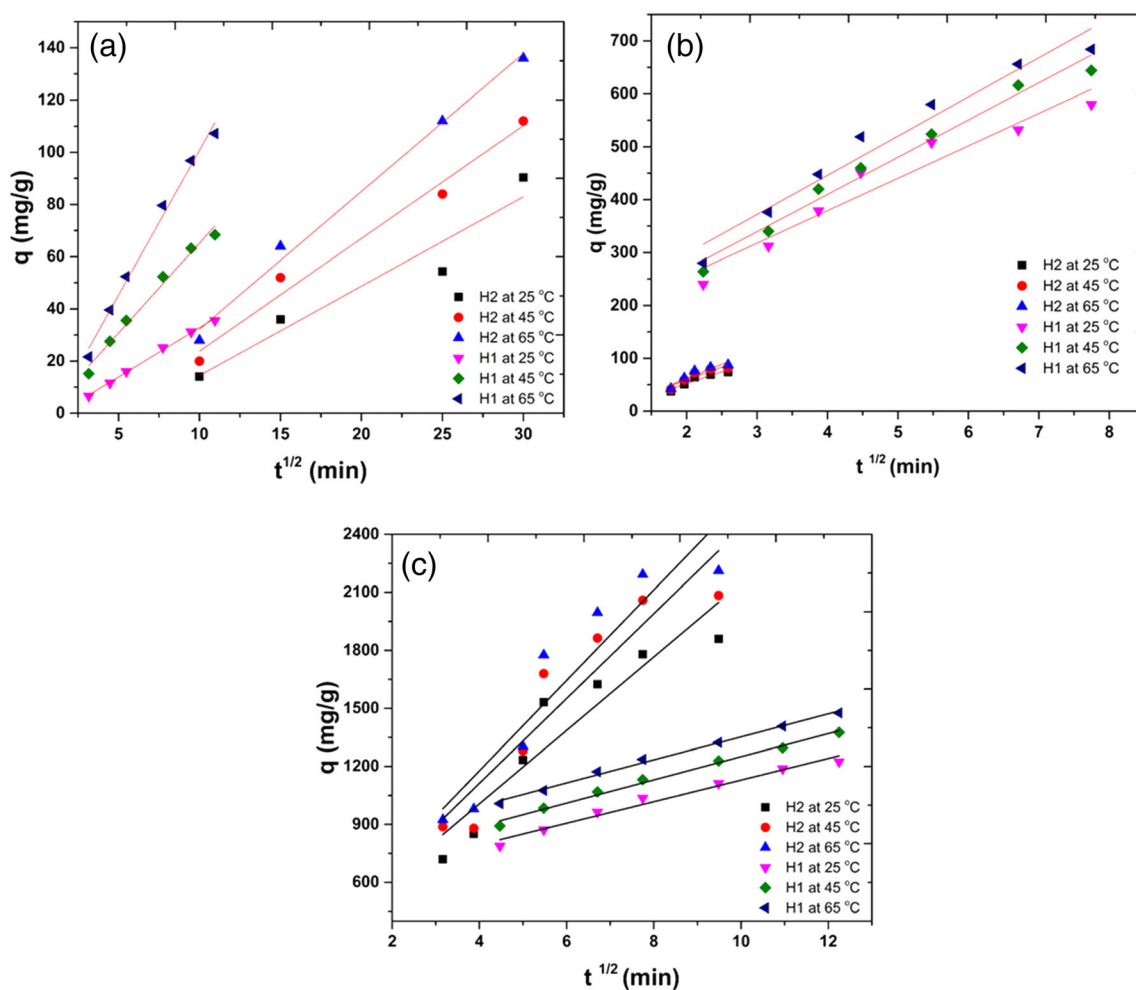


Figure 8. Intra-particle kinetic plots for the adsorption of (A) MB (concentration 40.0 mg L⁻¹ at pH 9.0), (B) FA (concentration 250.0 mg L⁻¹ at pH 5.0) and (C) CR (concentration 600.0 mg L⁻¹ at pH 7.0) onto **H1** and **H2** at different temperatures.

Table 5. Thermodynamic parameters for the adsorption of MB, FA and CR onto **H1** and **H2** at different temperatures

Dye/gel	Temperature (K)	ΔH° (kJ mol ⁻¹)	ΔS° (J·mol ⁻¹ ·K ⁻¹)	ΔG° (kJ mol ⁻¹)	E_a (kJ mol ⁻¹)
MB/H1	298.15	-18.565	0.086	-44.226	16.433
	318.15			-45.947	
	338.15			-47.669	
MB/H2	298.15	-30.696	0.105	-61.890	-10.319
	318.15			-63.983	
	338.15			-66.075	
FA/H1	298.15	-7.051	0.036	-17.961	5.071
	318.15			-18.692	
	338.15			-19.424	
FA/H2	298.15	-19.016	0.072	-40.594	4.891
	318.15			-42.041	
	338.15			-43.489	
CR/H1	298.15	-9.001	0.031	-18.123	1.078
	318.15			-18.734	
	338.15			-19.346	
CR/H2	298.15	-25.739	0.097	-54.543	6.464
	318.15			-56.475	
	338.15			-58.407	

Table 6. Adsorption/desorption for MB, FA and CR dyes onto hydrogel **H1** and **H2**

Gel	Cycle no.	Methylene blue		Fuchsin acid		Congo Red	
		q_e (mg g ⁻¹)	Desorption %S	q_e (mg g ⁻¹)	Desorption %S	q_e (mg g ⁻¹)	Desorption %S
H1	1	57.47	81.34	671.14	89.92	1351.35	90.61
	2	50.21	76.55	601.50	82.18	1109.43	86.32
	3	43.22	71.04	579.11	78.80	920.78	74.97
	4	40.39	66.63	498.21	75.66	816.44	71.12
H2	1	156.25	93.60	960.80	98.01	2380.39	94.01
	2	149.62	91.29	935.71	94.15	2178.76	90.44
	3	146.11	90.04	889.00	90.87	2007.05	86.02
	4	141.09	89.48	870.02	88.98	1956.06	80.43

indicating that the adsorption processes were endothermic. The positive values of the adsorption entropy (ΔS°) for the adsorption of MB, FA and CR onto the prepared hydrogels indicate an increase in the randomness at the adsorbent/solution interface and affinity of the prepared hydrogels towards these dyes.⁶⁰ The free energy change (ΔG°) values for the three dyes are negative and increase with increasing temperature, denoting that the adsorption processes proceed spontaneously and reversibly. The obtained ΔG° values are lower than 20 kJ mol⁻¹ indicating that the process follows the physisorption mechanism.^{68,69} The activation energy (E_a) values obtained are less than 40 kJ mol⁻¹ and this further supports the fact that the adsorption process follows the physisorption mechanism.

Desorption studies are essential to elucidate the reusability of an adsorbent, to understand the nature of the adsorption system and to evaluate the potential of recycling. Table 6 shows that the desorption percentages of **H2** in the fourth cycle were 89.48%, 88.98% and 80.43% for MB, FA and CR respectively. In contrast, the percentage of desorption values of **H1**, the control, were 66.36%, 75.66% and 71.12% for MB, FA and CR respectively. This clearly demonstrates that the **H2** hydrogel adsorbent can be used multiple times whilst retaining a high adsorption capacity.

CONCLUSION

In conclusion, the efficient removal of the dyes MB, FA and CR from aqueous solutions was observed when using the hydrogels **H1** and **H2** as adsorbents. The maximum adsorption of MB, FA and CR onto the prepared hydrogels was obtained at pH 5.0, 7.0 and 9.0 respectively. The adsorption systems of all dyes were found to increase with increase in temperature and fitted the Langmuir model, which allowed us to predict the chemical mechanism of the adsorption systems. From the linearised form (from the calculation of the Langmuir equation (q_{max})), values for the MB, FA and CR dyes were 769.20, 1666.70 and 2358.20 mg g⁻¹ respectively, which exceed many of the reported values in the literature.^{37,53–59} Depending on the values of the correlation coefficient, the pseudo-first-order kinetic model indicated the adsorption kinetics of the MB and FA dyes, whereas the pseudo-second-order kinetic model accurately indicated the adsorption kinetics of the CR dye on the prepared hydrogel **H2**. The derived thermodynamic parameters from this study are indicative of a physisorption process; thus, the adsorption processes could have chemical and physical behaviour. Excellent regeneration efficiency is observed for hydrogels **H1** and **H2** over four successive

adsorption cycles. The desorption percentages at the fourth cycle for H2 were 89.48%, 88.98% and 80.43% for the MB, FA and CR dyes respectively, thereby making the removal process of these toxic dyes more economical. The newly synthesised hydrogels of PePnUMA-co-AMPS along with acrylamide, HEMA and N-isopropylacrylamide exhibit an enhanced adsorption capacity.

ACKNOWLEDGEMENT

A. A. Alwattar gratefully acknowledges the Iraqi Ministry of Higher Education and Scientific Research (MOHER) and the University of Basrah (Chemistry Department) for the provision of a research sabbatical. M. Alshareef thanks the Ministry of Higher Education of Saudi Arabia and Umm Al-Qura University for funding.

REFERENCES

- David Noel S and Rajan MR, *J Pollut Eff Control* **02**:1–4 (2014).
- Raymond S, Mathias V and Henry D, *Science* **312**:1755–1756 (2006). Available: science.sciencemag.org.
- Carneiro P, Umbuzeiro G, Oliveira D and Zanoni M, *J Hazard Mater* **174**:694–699 (2010).
- Chen K, Wu Y, Huang C, Liang Y and Hwang S, *J Biotechnol* **101**:241–252 (2003).
- Pandey S, Do J, Kim J and Kang M, *Int J Biol Macromol* **143**:60–75 (2020).
- Yaseen D and Scholz M, *Environ Sci Pollut Res* **25**:1980–1997 (2018).
- Yao L, Yang H, Chen Z, Qiu M, Hu B and Wang X, *Chemosphere*:1–19 (2020). <https://doi.org/10.1016/j.chemosphere.2020.128576>
- Hu B, Ai Y, Jin J, Hayat T, Alsaedi A, Zhuang L et al., *Biochar* **2**:47–64 (2020).
- Alharbi NS, Hu B, Hayat T, Rabah SO, Alsaedi A, Zhuang L et al., *Front Chem Sci Eng* **14**:1124–1135 (2020).
- Hao M, Qiu M, Yang H, Hu B and Wang X, *Sci Total Environ* **760**:1–26 (2020).
- Mouni L, Belkhir L, Bollinger J, Bouzaza A, Assadi A, Tirri A et al., *Appl Clay Sci* **153**:38–45 (2018).
- Shalla A, Bhat M and Yaseen Z, *J Environ Chem Eng* **6**:5938–5949 (2018).
- Gu J, Chen H, Jiang F and Wang X, *J Colloid Interface Sci* **540**:97–106 (2019).
- Wei N, Zheng X, Ou H, Yu P, Li Q and Feng S, *New J Chem* **43**:5603–5610 (2019).
- Mall D, Srivastava C, Agarwal K and Mishra M, *Chemosphere* **61**:492–501 (2005).
- Rani C, Naik A, Chaurasiya S and Raghavarao S, *Water Sci Technol* **75**:2225–2236 (2017).
- Mittal A, Mittal J, Malviya A and Gupta K, *J Colloid Interface Sci* **340**:16–26 (2009).
- Foroughi-Dahr M, Abolghasemi H, Esmaili M, Shojamoradi A and Fatoorehchi H, *Chem Eng Commun* **202**:181–193 (2015).
- Jana S, Pradhan S and Tripathy T, *J Polym Environ* **26**:2730–2747 (2018).
- Üzümlü B, Bayraktar İ, Kundakç S and Karadağ E, *Polym Bull* **77**:847–867 (2020).
- Dragan S, *Chem Eng J* **2014**:572–590 (2014).
- Thakur K, Gels Horizons: From Science to Smart Materials, in *Hydrogels*, ed. by Thakur K. Springer Singapore, Singapore (2018). <https://doi.org/10.1007/978-981-10-6077-9>.
- Dey E, Wimpenny I, Gough E, Watts C and Budd M, *J Biomed Mater Res Part A* **106**:255–264 (2018).
- Laftah A, Hashim S and Ibrahim N, *Polym Plast Technol Eng* **50**:1475–1486 (2011).
- Jv X, Zhao X, Ge H, Sun J, Li H, Wang Q et al., *J Chem Eng Data* **64**:1228–1236 (2019).
- Nakhjiri T, Marandi B and Kurdtabar M, *Int J Biol Macromol* **117**:152–166 (2018).
- Moore J, Raine P, Jenkins A, Livens R, Law A, Morris K et al., *React Funct Polym* **142**:7–14 (2019).
- Abdulmonaim Z and Haddad A, *Drug Des Intellect Prop Int J* **1**:55–63 (2018).
- Shakoor S, Nasar A and Taiwan Inst J, *Chem Eng* **66**:154–163 (2016).
- Hassanpour M, Safardoust-Hojaghan H and Salavati-Niasari M, *J Mol Liq* **229**:293–299 (2017).
- Moradi E, Ebrahimzadeh H, Mehrani Z and Asgharinezhad A, *Environ Sci Pollut Res* **26**:35071–35081 (2019).
- Asses N, Ayed L, Hkiri N and Hamdi M, *Biomed Res Int* **6**:3049686 (2018).
- Sakkas V, Islam A, Stalikas C and Albanis A, *J Hazard Mater* **175**:33–44 (2010).
- Klaus H, Peter M, Wolfgang R, Roderich R and Klaus E, *Encyclopedia of Industrial Chemistry*. Wiley-VCH, Weinheim, pp. 1–24 (2005).
- Mustroph H, Dyes, general survey, in *Ullmann's Encyclopedia of Industrial Chemistry*. Wiley-VCH, Weinheim, pp. 1–38 (2014).
- Jing P, Li J, Pan L, Wang J, Sun X and Liu Q, *J Hazard Mater* **284**:163–170 (2014).
- Xing J, Yang B, Shen Y, Wang Z, Wang F, Shi X et al., *J Dispers Sci Technol* **40**:1591–1599 (2019).
- Kalkan E, Nadaroglu H, Celebi N, Celik H and Tasgin E, *Polish J. Environ Stud* **24**:115–124 (2015).
- Zhang Q, Hu M, Wu Y, Wang M, Zhao Y and Li T, *React Funct Polym* **136**:34–43 (2019).
- Tanzil R, Luqman S, Mansoor K and Khattak N, *RSC Adv* **9**:18565 (2019).
- Agnihotri S and Singhal R, *J Polym Environ* **27**:372–385 (2019).
- Alwattar A, Haddad A, Moore J, Alshareef M, Bartlam C, Woodward A et al., *Polym Int* **70**:59–72 (2021).
- Alwattar A, Haddad A, Zhou Q, Nascimento T, Greenhalgh R, Medeiros E et al., *Polym Int* **68**:360–368 (2019).
- Al-attar H, Alwattar A, Haddad A, Abdullah B and Yeates S, *Polym Int* **70**:51–58 (2021).
- Yilmaz E, Guzel Kaya G and Devci H, *J Polym Sci Part A Polym Chem* **57**:1070–1078 (2019).
- Singha R, Dutta A, Mahapatra M, Roy D, Mitra M, Deb M et al., *ACS Omega* **4**:1763–1780 (2019).
- Soldatkina L and Zavrlichko M, *Colloids Interfaces* **3**:4 (2018).
- Weber M, *Allergo J Int* **23**:200–200 (2014).
- Nakhjiri T, Bagheri Marandi G and Kurdtabar M, *J Polym Environ* **27**:581–599 (2019).
- Zhou J, Hao B, Wang L, Ma J and Cheng W, *Sep Purif Technol* **176**:193–199 (2017).
- Yan K, Yuan Z, Zhiyong H, Jianwei Y, Baoyou S and Kun H, *J Environ Sci* **78**:81–91 (2019).
- Adeyi A, Jamil M, Abdullah C, Choong Y, Lau L and Abdullah M, *Materials (Basel)* **12**:1734–1750 (2019).
- Chatterjee S, Chatterjee S, Chatterjee P and Guha K, *Colloids Surf A Physicochem Eng Asp* **299**:146–152 (2007).
- Wang P, Yan T and Wang L, *BioResources* **8**:6026–6043 (2013).
- Chatterjee S, Lee S, Lee W and Woo H, *Bioresour Technol* **100**:2803–2809 (2009).
- Zhou X, Zheng P, Wang L and Liu X, *Polymers (Basel)* **11**:32–48 (2018).
- Bao S, Wu D, Wang Q and Su T, *PLoS One* **9**:1–8 (2014).
- Wang Z, *Sci Rep* **7**:7878 (2017).
- Dahlan A, Lee W, Pushpamalar J and Ng L, *Int J Environ Sci Technol* **16**:2047–2058 (2019).
- Bhattacharyya R and Ray K, *Chem Eng J* **260**:269–283 (2015).
- Canossa S, Predieri G and Graiff C, *Acta Crystallogr Sect E Crystallogr Commun* **74**:587–593 (2018).
- Appusamy A, Purushothaman P, Ponnusamy K and Ramalingam A, *J Thermodyn* **2014**:1–17 (2014).
- Hoslett J, Ghazal H, Mohamad N and Jouhara H, *Sci Total Environ* **714**:136832 (2020).
- Saadi R, Saadi Z, Fazaeli R and Fard E, *Korean J Chem Eng* **32**:787–799 (2015).
- Karagöz S, Tay T, Ucar S and Erdem M, *Bioresour Technol* **99**:6214–6222 (2008).
- Kaur K, Jindal R and Saini D, *Polym Bull* **77**:3079–3100 (2020).
- Erdem M, Yüksel E, Tay T, Çimen Y and Türk H, *J Colloid Interface Sci* **333**:40–48 (2009).
- Malana A, Ijaz S and Ashiq N, *Desalination* **263**:249–257 (2010).
- Zhang Y, Yu F, Cheng W, Wang J and Ma J, *J Chem.* **2017**:1–9 (2017).